Vol. 105 No. 3 March 2008

Oral Surgery, Oral Medicine, Oral Pathology, Oral Radiology, and Endodontology

ORAL AND MAXILLOFACIAL RADIOLOGY Editor: Allan G. Farman

Bisphosphonate-associated jawbone osteonecrosis: a correlation between imaging techniques and histopathology

Alberto Bedogni, MD,[a] Stella Blandamura, MD,[b] Zerina Lokmic, MD,[c] Carla Palumbo, MD,[d] Mirko Ragazzo, MD,[e] Francesca Ferrari, MD,[a] Alberto Tregnaghi, MD,[f] Francesco Pietrogrande, MD,[g] Olindo Procopio, MD,[e] Giorgia Saia, MD,[e] Marzia Ferretti, MD,[d] Giorgio Bedogni, MD,[h] Luigi Chiarini, MD,[i] Giuseppe Ferronato, MD,[e] Vito Ninfo, MD,[b] Lucio Lo Russo, DDS, PhD,[j] Lorenzo Lo Muzio, MD, PhD,[j] and Pier Francesco Nocini, MD, DDS,[a] Verona, Padova, Modena, Reggio Emilia, Trieste, and Foggia, Italy; and Meunster, Germany

UNIVERSITY OF VERONA, UNIVERSITY OF PADOVA, UNIVERSITY OF MODENA AND REGGIO EMILIA, LIVER RESEARCH CENTER, UNIVERSITY OF FOGGIA, AND UNIVERSITY OF MUENSTER

Objectives. Recently, jawbone osteonecrosis has been reported as a potential adverse effect of bisphosphonates administration. This paper considers and highlights histopathologic and radiologic features of this condition.
Study design. Eleven patients, owing to unresponsiveness to conservative treatment and uncontrollable pain, underwent surgical resection of diseased jawbone after extensive hyperbaric oxygen therapy. A thorough clinical, laboratory, and imaging study was performed. Surgical specimens underwent histopathologic and immunohistochemical evaluation.
Results. Computerized tomography (CT) scans showed increased bone density, periosteal reaction, and bone sequestration in advanced stages. With magnetic resonance imaging (MRI), exposed areas showed a low signal in T1- and T2-weighted and inversion recovery images, which suggests low water content and is histopathologically correlated with paucity in cells and vessels (osteonecrotic pattern). Unexposed diseased bone was characterized by T1 hypointensity and T2 and IR hyperintensity, which suggests high water content and inflammation, associated with hypercellularity, osteogenesis, and hypervascularity (osteomyelitic pattern).
Conclusions. Diseased bone extends beyond the limits of the bone exposed in the oral cavity. Histopathologic examination correlated well with CT and MRI, which are the choice for the evaluation of bisphosphonate-associated jawbone osteonecrosis. **(Oral Surg Oral Med Oral Pathol Oral Radiol Endod 2008;105:358-64)**

Aminobisphosphonates play a central role in the treatment of malignancy-associated hypercalcemia and for the prevention of bone fractures in patients with metastatic bone disease or multiple myeloma.[1-3] Among aminobisphosphonates, pamidronate and zoledronate have shown the most consistent effects for the treatment of bone metastases in cancer, with zoledronate being more potent in vitro than pamidronate.[4] Aminobisphosphonates inhibit osteoclasts at different stages, binding selectively to hydroxyapatite and accumulating in sites of active bone remodeling. Once bisphosphonates are stored in bone, their release is dependent on the rate of bone remodeling.[5] In addition, aminobisphosphonates have antiangiogenic properties both in vitro and in vivo.[6,7]

[a]Unit of Dentistry and Maxillofacial Surgery, University of Verona.
[b]Institute of Pathology, University of Padova.
[c]Institute of Physiological Chemistry and Pathobiochemistry, University of Muenster.
[d]Department of Anatomy and Histology, University of Modena and Reggio Emilia.
[e]Unit of Maxillofacial Surgery, University of Padova.
[f]Institute of Radiology, University of Padova.
[g]Department of Medical and Surgical Sciences, University of Padova.
[h]Liver Research Center, Area Science Park, Basovizza, Trieste.
[i]Unit of Dentistry and Maxillofacial Surgery, University of Modena and Reggio Emilia.
[j]Department of Surgical Sciences, University of Foggia.
Received for publication Jun 21, 2007; returned for revision Jul 31, 2007; accepted for publication Aug 30, 2007.
1079-2104/$ - see front matter

doi:10.1016/j.tripleo.2007.08.040

Table I. Clinical data of patients

Case	Age	Gender	Underlying malignancy	Bisphosphonate	Bisphosphonate duration (months)	Other drugs	Affected jaw	Precipitating event
1	75	F	Multiple myeloma	Pamidronate/zoledronate	24	Thalidomide melphalan, prednisone	Mandible	Prosthesis
2	49	F	Breast cancer	Pamidronate/zoledronate	9	Aromatase inhibitor	Mandible	Tooth extraction
3	56	F	Breast cancer	Pamidronate/zoledronate	36	None	Mandible	Tooth extraction
4	74	M	Kidney cancer	Pamidronate/zoledronate	12	Vinblastin, gemcitabin, prednisone	Mandible	Tooth extraction
5	65	M	Multiple myeloma	Zoledronate	18	Vincristine, adriamycin, dexamethason	Mandible	Tooth extraction
6	84	F	Multiple myeloma	Pamidronate/zoledronate	60	None	Maxilla	Tooth extraction
7	65	F	Breast cancer	Pamidronate/zoledronate	60	Palliation chemotherapy	Maxilla	Spontaneous
8	70	F	Breast cancer	Pamidronate/zoledronate	48	Aromatase inhibitor	Maxilla	Tooth extraction
9	79	F	Multiple myeloma	Pamidronate/zoledronate	48	None	Mandible	Tooth extraction
10	72	M	Prostate cancer	Zoledronate	36	Bicalutamide	Mandible	Spontaneous
11	64	M	Multiple myeloma	Pamidronate	12	Dexametasone, interferon	Mandible	Tooth extraction

Recent studies performed in cancer patients suggest that bisphosphonates, in some cases, may be responsible for jawbone lesions.[8-10] Clinically, these lesions appear as nonhealing exposed bone areas, which can be accompanied by fistulization, purulent discharge, and pain.[11-14] The current nomenclature for bisphosphonate-associated jawbone lesions reflects the prevailing hypothesis that such a condition is a form of osteonecrosis.[11,15,16] However, the pathogenesis of jawbone disease in patients receiving bisphosphonates is largely unknown, and the biologic mechanisms by which bisphosphonates are responsible for bone remodeling and angiogenesis impairment in human jaws are still uncertain. Furthermore, very few data are available in the literature regarding histopathologic and radiologic features. In the present paper, we have addressed and reported data regarding histopathology and radiologic features of bisphosphonate-associated jaw osteonecrosis that occurred in a series of our patients.

METHODS

Patients

The study group (Table I) consisted of 11 patients (4 men and 7 women) whose ages ranged from 49 years to 84 years (mean age 75.9 years). Five patients (45.5%) were affected by multiple myeloma, 4 (36.4%) by breast cancer, 1 (9%) by prostate cancer, and 1 (9%) by kidney cancer. All of them received intravenous aminobisphosphonates for a mean period of 37.3 months (range 9 months to 60 months); in particular, 1 patient received pamidronate, 1 received zoledronate, and the remaining 9 were first administered with pamidronate and then with zoledronate. Eight patients also received concomitant therapy for the underlying malignancy as detailed in Table I. All patients developed jawbone osteonecrosis. It occurred in 2 cases without apparent precipitating events, and in 8 patients a history of tooth extraction was reported, whereas in 1 patient a trauma from poorly fitting removable denture was identified; the mandible and the maxilla were affected in 8 cases (73%) and 3 cases (27%), respectively. Owing to unresponsiveness to conservative treatment (antibiotics + superficial surgical debridement) and uncontrollable pain, in accordance with the oncologists and with patient's consent, it was decided to perform surgical resection of the affected area of jawbone. Preoperatively, a thorough clinical, laboratory, and imaging technique study of patients was performed.

Radiologic evaluation

Patients underwent panoramic radiograph, spiral computerized tomography (CT), and magnetic resonance imaging (MRI) of the jaws. The CT scans (CT Brilliance 6 slices; Philips), based on 1-mm to 2-mm axial slices parallel to the hard palate, were evaluated with wide windowing levels. True cross-sectional images of the mandible and maxilla were obtained from CT data using multiplanar reformation software (Denta-scan®). No contrast media were used for CT imaging.

The MRI images of the jaws were obtained by using a magnet of 1.5 T (Magnetom Symphony 1.5 Tesla; Siemens). The MRI scans consisted of T1- and T2-weighted spin-echo axial and inversion recovery (IR) images, 4 mm in thickness and at 0.4-mm intervals.

Treatment

After discontinuation of bisphosphonates therapy, a 10-day cycle of antibiotic therapy (amoxicillin-clavu-

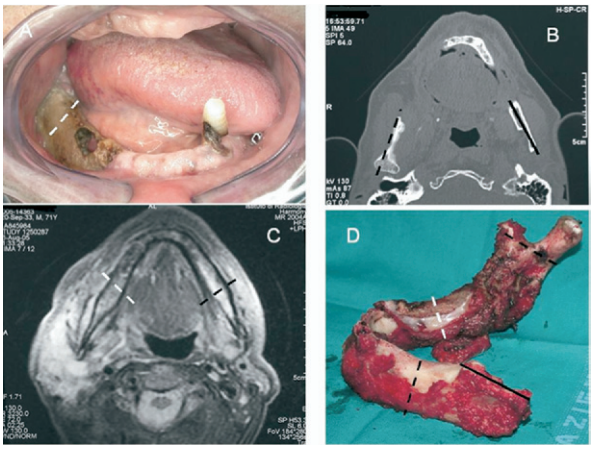

Fig. 1. **A,** Intraoral view of an extensive right mandibular bone exposure; **B,** preoperative axial CT scan showing extension of disease to the right mandibular condyle and healthy bone in the left ascending ramus; **C,** preoperative MRI (IR sequence) showing low signal intensity on the right mandibular body and high signal intensity on the left mandibular body; **D,** surgical specimen after subtotal mandibulectomy including the right condylar head.

lanate and metronidazole) was prescribed. Furthermore, all patients underwent 25 preoperative sessions of hyperbaric oxygen therapy (HBO) (2.5 ATA, 90 minutes), and then a complete resection of the diseased bone with jaw reconstruction if needed was performed. Postoperatively, patients received a 10-day cycle of antibiotic therapy and 25 sessions of HBO.

Histopathology and immunohistochemistry

The specimens of the 11 patients who underwent bone resection were histopathologically evaluated. Every specimen was cut to obtain multiple bone sections consisting of the entire cross-sectional area of the resected jaw. The periosteal layer was included. Sampling for histopathologic evaluation was performed from areas with bone exposed in the oral cavity, from each margin of bone resection, and from areas of diseased bone but without intraoral exposure (Fig. 1).

Specimens were fixed in 4% formaldehyde, decalcified in Kristensen solution for 24-48 hours,[17] and embedded into paraffin blocks. Tissue blocks were cut into 5-μm serial sections, stained with hematoxylin and eosin, and photographed (Leica DFC 280; Leica Microsystems Imaging Solution, Cambridge, U.K.). Immunohistochemical staining was used to evaluate blood vessels within specimens. In particular, specimens were subjected to immunoperoxidase stains (CD34 antibody clone QBEND 10, dilution 1:40; Immunotech, Marseilles, France) according to the manufacturer's instructions.

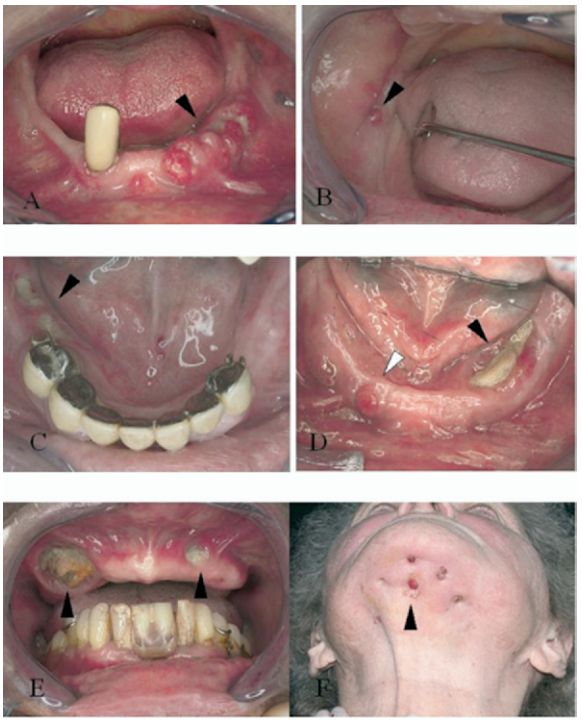

Fig. 2. Clinical presentation of the bisphosphonate-associated jawbone disease: **A)** Infected postextraction sockets; **B,** fistula of the retromolar area; **C,** early bone exposure of the retromolar area; **D,** extensive exposure of necrotic bone (*black arrowhead*) accompanied by gingival fistulization on the opposite side (*white arrowhead*) in an advanced case; **E,** bilateral exposure of necrotic bone in an edentulous maxilla; **F,** multiple secreting submental fistulas with gross deformity of the lower third of the face.

RESULTS

Clinically, bone disease presented as a nonhealing extraction socket or areas of extensive bone exposure (9 patients) with variable purulent discharge (Fig. 2, *A*). Gingival fistulae were sometimes observed (Fig. 2, *B-E*) as well as cervical cutaneous fistulae in advanced bone disease (Fig. 2, *F*).

Radiologic findings

Panoramic radiographs showed delayed or absent bone remodeling of the extraction sockets (Fig. 3, *A*). Diffuse radiopaque areas were seen between radiolucent areas in advanced bone disease.

The CT scans showed large areas of increased medullary bone density extending beyond the limits of the bone exposed in the oral cavity (Fig. 3, *B*). Periosteal reaction and bone sequestration were predominant in advanced stages of disease (Fig. 3, *C*). Maxillary involvement was always associated with purulent sinusitis. The entire cross-sectional area of the jaw was involved in all cases (Fig. 3, *D*).

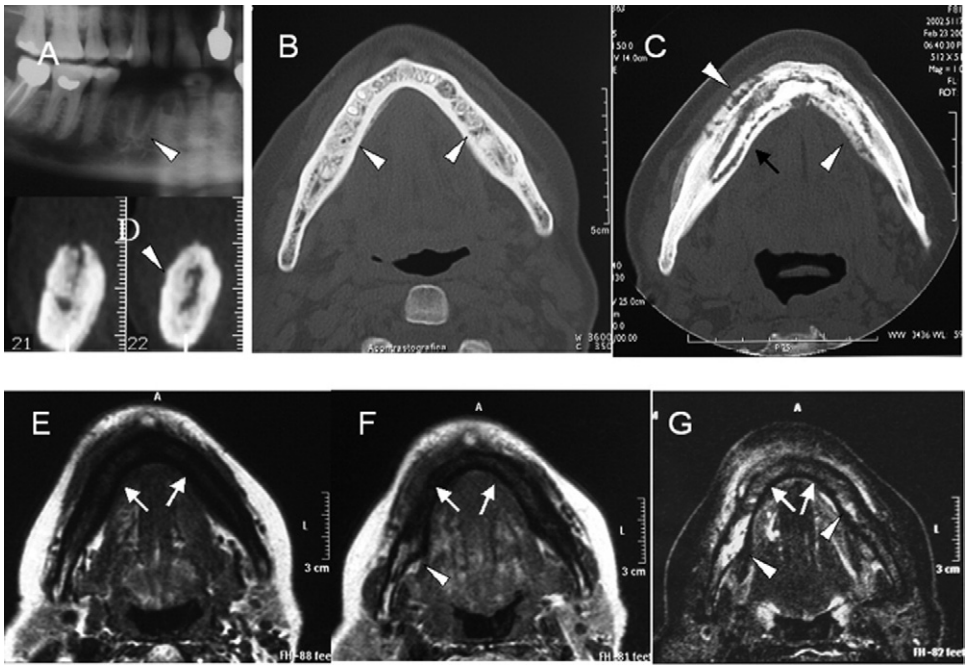

Fig. 3. Radiologic features of the bisphosphonate-associated jawbone disease: **A,** panoramic radiograph (detail) showing post-extraction sockets without signs of bone remodeling at 6-month follow-up (*white arrowhead*); **B,** CT scan: early mandibular bone disease with diffuse osteosclerosis (*white arrowhead*); **C,** CT scan: extensive periosteal reaction (*white arrowhead*) and large bone sequestration (*black arrow*) in a case of advanced mandibular disease; **D,** Denta-scan: increased medullary and cortical bone density; **E-G,** MRI sequence (T1, T2, IR, respectively) showing coexisting patterns of necrosis (*white arrows*) and inflammation (*white arrowheads*) in the same jaw.

The MRI showed 2 patterns of bone disease in the studied cases. In the first pattern, characteristic of exposed areas of diseased bone, low signal was observed in T1- and T2-weighted images, with a relatively low signal in IR images, which was suggestive of low water content. The second pattern, typical of unexposed diseased bone, was characterized by T1 hypointensity and T2 and IR hyperintensity, suggesting high water content (Fig. 3, *E-G*). In advanced disease with extensive bone exposure, the 2 patterns coexist, with the second one being always present in a peripheral distribution (Fig. 3, *E-G*).

Histopathologic findings

The specimens obtained from the areas of exposed bone in the oral cavity were characterized by a large amount of nonvital bone, with rough margins and empty lacunae. Osteoblasts and multinucleated osteoclast-like cells were almost absent and vessels were scanty, no sign of bone remodeling was seen. Fungal contamination of the exposed necrotic bone was found in most cases. In contrast, the specimens obtained from the areas of diseased but unexposed bone were characterized, in all of the resected jaws, by hypervascular fibrous tissue and inflammatory infiltrate filling large intertrabecular spaces. Areas of lamellar bone with empty lacunae coexisted with areas of lamellar bone containing viable osteocytes surrounded by woven-fiber bone. In all cases, woven bone largely prevailed over lamellar bone (Figs. 4, *A* and *B*). At sites where osteogenesis was evident, bone trabeculae were rimmed by osteoblasts (Fig. 4, *C*). The formation of new bone was also detected below the periosteum (Fig. 4, *D*). In all of the specimens, intertrabecular spaces were rich in blood vessels of different size and multinucleated osteoclast-like cells detached from the bone surface (Fig. 4, *E*). The specimens obtained from the margins of resection showed normal bone structure and vasculature in 8 out of 11 jaws (Fig. 4, *F*). Three patients showed moderate signs of osteomyelitis at one margin of bone resection.

The vasculature of the affected tissue was constituted by a mixture of capillaries, round venule-like vessels, and small arterioles (Fig. 5, *A*). The capillaries had normal histologic features. Most CD34-positive arterioles within the fibrous tissue had a rounded or slightly cuboidal endothelium (Fig. 5, *B*), very similar to the picture observed in chronic osteomyelitis (Fig. 5, *F*). Most vessels contained pink proteinaceous material in their lumen and red blood cells agglutinated into a roleaux, which is probably a post-biopsy fixation artifact (Fig. 5, *C* and *D*).

DISCUSSION

In this study we evaluated and reported the radiologic features in a series of jawbones resected from patients affected by bisphosphonate-associated jaw-

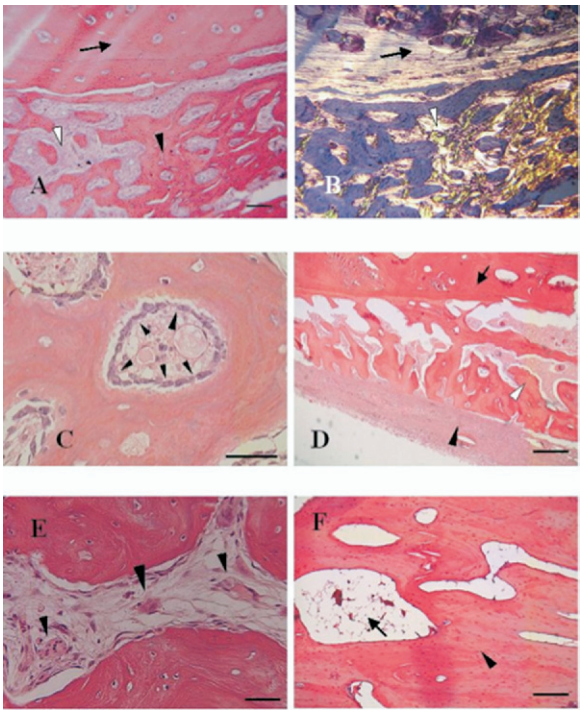

Fig. 4. Histopathologic features of the bisphosphonate-associated jawbone disease: **A,** osteogenic pattern of the disease (no intraoral exposure): new trabecular bone and viable osteocytes (*black arrowhead*), large intertrabecular spaces filled with highly vascularized fibrous tissue (*white arrowhead*) with a clear demarcation from adjacent unaffected bone (*black arrow*) (H&E stain; scale bar: 250 μm); **B,** polarized light micrograph of the same field as in *A* (scale bar: 250 μm): woven-fiber bone (*white arrowhead*) prevails over lamellar bone; **C,** secreting osteoblastic lamina (*black arrowheads*) surrounding a wide round-shaped intertrabecular space (H&E stain; scale bar: 20 μm); **D,** periosteal reaction: new bone formation bordered by soft tissues (*black arrowhead*) and cortical bone (*black arrow*) (H&E stain; scale bar: 500 μm); **E)** intertrabecular space with multinucleated osteoclast-like cells (*black arrowheads*) detached from the bone surface (H&E stain; scale bar: 50 μm); **F,** bone resection margin showing regular bone architecture (*black arrowhead*) with adipose tissue infiltrates in the medullary spaces (*black arrow*) (H&E stain; scale bar: 500 μm).

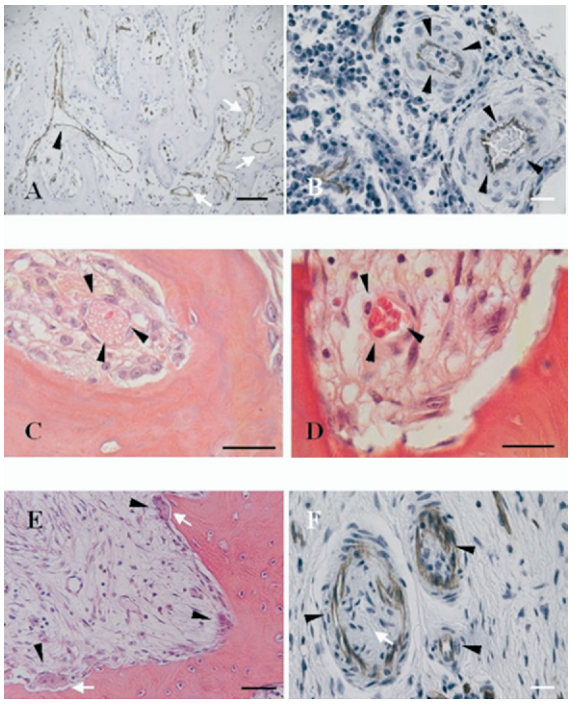

Fig. 5. Histopathologic features of bisphosphonate-associated jawbone disease: **A**) vascularized tissue with vessel branching visible in the intertrabecular spaces (*black arrowhead*) (CD34 stain; scale bar: 100 μm); **B**) diseased tissue showing arterioles with hypertrophic muscle wall, narrow lumen, and slightly cuboidal endothelium (*black arrowheads*) (CD34 stain; scale bar: 20 μm); **C**) pink proteinaceous material (*black arrowheads*) is seen inside the lumen of blood vessels (H&E stain; scale bar: 25 μm); **D**) red blood cells agglutinating into roleaux inside small vessels (*black arrowheads*) (H&E stain; scale bar: 25 μm); **E**) specimen obtained from the mandible of a patient with primary chronic osteomyelitis. Note the 3 eroding osteoclasts (*black arrowheads*) close to Howship lacunae (*white arrows*) (H&E stain; scale bar: 50 μm); **F**) specimen obtained from the mandible of a patient with primary chronic osteomyelitis. The 3 arterioles within the intertrabecular space have a slightly cuboidal endothelium (*black arrowheads*) and a narrow lumen almost occluded by viscous material (*white arrow*) (CD34 stain; scale bar: 20 μm).

bone disease; furthermore, we have attempted to define their related histopathologic features.

Bisphosphonate-associated jawbone disease encompasses a number of alterations involving macroscopic anatomy of jawbones, bone structure, bone cell populations and function, and vasculature. Modifications in bone morphology are clearly visible both from a clinical point of view and at CT scan (Figs. 2 and 3). It should be emphasized that the diseased bone goes much beyond the limits of the clinically exposed bone areas, and therefore clinical examination is not at all reliable in assessing lesion extent. Both CT scan and MRI are adequate in evaluating bone involvement, as confirmed by previous studies.[18] The CT features of jawbone disease resembled those of a chronic osteomyelitic process, with predominant signs of osteosclerosis and periosteal reaction; osteolysis may be also evident, in accordance with other authors.[18]

Diseased bone is always involved in all of its cross-section, including the periosteum, as confirmed by both cross-sectional reformatted images and histopathologic sections. In addition, diseased bone exhibits different features resulting from being exposed in the oral cavity or not. This was not reported in other studies,[18] but in the

Table II. Histopathology of bisphosphonate-associated osteonecrosis and imaging features correlates

		Exposed affected bone	*Unexposed affected bone*
CT scan			Increased medullary bone density Thickening of trabeculae Periosteal reaction Bone sequestration (advanced stages)
MRI		Low T1- and T2-weighted signal Low signal in IR	T1 hypointensity T2 and IR hyperintensity
Histopathology	Intertrabecular spaces	Empty	Large intertrabecular spaces Hypervascular fibrous tissue Inflammatory infiltrate
	Cell populations	Osteoblasts and multinucleated osteoclast-like cells almost absent	Osteoblasts rim new bone trabeculae Multinucleated osteoclast-like cells detached from the bone surface
	Vasculature	Almost absent	Capillaries Round venule-like vessels Small arterioles (rounded or slightly cuboidal endothelium) Pink proteinaceous endoluminal material Red blood cells agglutinated into a roleaux

IR, Inversion recovery.

present series it is evident at MRI investigation and is further confirmed at a microscopic level by histopathologic examination. The first MRI pattern described above, suggestive of low water content, is typically associated with the areas of bone exposed in the oral cavity, whereas the second MRI pattern, suggestive of edema and inflammation, characterizes unexposed areas. These MRI patterns have specific histopathologic correlates (Table II). Paucity in cells and vessels is typically seen in the areas of exposed bone, making up the picture of necrosis; on the other hand, diseased but unexposed bone is characterized by hypercellularity, hypervascularity, and osteogenesis: histopathologic aspects that are also characterizing but not exclusive features of osteomyelitis. In particular, new bone trabeculae rimmed by osteoblasts and delimiting large intertrabecular spaces filled by hypervascular fibrous tissue and inflammatory infiltrate well fit the histopathologic picture of a chronic osteomyelitic process, but the same does not apply to multinucleated osteoclast-like cells. They are typically detached from the bone surface (Fig. 4, *E*), whereas in chronic osteomyelitis the osteoclasts are attached to bone and show erosive activity (Fig. 5, *E*). This detachment is of special interest because it gives us the opportunity to hypothesize that these multinucleated osteoclast-like cells are effectively osteoclasts whose alterations in cellular morphology can be attributed just to loss of bone contact; on the other hand, their detachment from bone may well reflect the functional impairment caused by bisphosphonates. In fact, it is well known that a key early event for bone resorption to be initiated is the attachment of the osteoclast to the bone matrix[19] via integrins (mainly $\alpha V\beta 3$), which results in the formation of the sealing zone that enables the osteoclast to isolate the subcellular resorptive microenvironment.[20] Aminobisphosphonates inhibit the mevalonate pathway and prevent post-translational prenylation of guanosine triphosphate–binding proteins,[21] including Ras, Rac, and Rho; this causes unbalance in function of these proteins which regulates the assembly of focal adhesions[22] and membrane ruffling[23] and are involved in bone resorption by regulating cytoskeletal organization in osteoclasts.[24] These events lead to alterations in cellular morphology and function and end up with the observed detachment of osteoclasts from bone, which may have a role in light of new proposed pathogenetic theories.[25]

Furthermore, we found histologic evidence of osteoclasts' inactivation in bisphosphonate-associated jawbone disease in all of the studied specimens. It is well known that bone homeostasis depends on the maintenance of a balanced activity between osteoblasts and osteoclasts; when bone resorption is decreased through inhibition of osteoclasts, the bone matrix is not degraded and nonvital bone accumulates.[5] Therefore, the presence of lamellar bone with empty lacunae seen within the osteomyelitic pattern may be explained by the accumulation of nonvital bone due to dysfunction of osteoclasts.

Blood vessel abnormalities involve their number, type, and structure; they are confined to the unexposed areas, because in the exposed ones vasculature is almost absent whereas the resection margins showed normal bone and vessels. Whether these vessel abnormalities are related to inflammation or impaired angiogenesis and vascularization remains to be determined. In addition, in the present series patients preoperatively underwent HBO therapy; it is well known that hyperbaric oxygen possesses significant angiogenic potential[26] and therefore may have con-

tributed to the hypervascularization seen in the osteomyelitic part of the resected jawbones. On the other hand, hypervascularization may seem not to fit with bisphosphonates' antiangiogenetic effect, but discontinuation of bisphosphonates in the present patients may have had a role in minimizing this effect.

Vascularization has been indicated among etiopathogenetic factors of bisphosphonate-associated bone disease; it has been postulated that the mandible may be especially susceptible to it because of its terminal vascularization.[13] In the present study, in agreement with others,[11,27] most bone lesions associated with bisphosphonate therapy were localized in the mandible (73% of cases); however, no histopathologic differences in vessels appearance were found between mandible and maxilla.

CONCLUSIONS

In conclusion, histopathologic examination correlated well with CT and MRI, which are the choice for the evaluation of bisphosphonate-associated jawbone osteonecrosis; in particular, bone alterations exhibit great variation between exposed and unexposed areas. The former express the features of an osteonecrotic process, whereas the latter resemble in many aspects an ostemyelitic one; if there is a continuous progression from the osteomyelitic to the osteonecrotic pattern, as observed in the avascular osteonecrosis of epiphyseal bone, it cannot be determined with the present data, probably because bone resection was decided when the bone exposure was sufficiently advanced and the necrotic bone had already separated from its osteomyelitic bed. MRI may have a special value in assessing and characterizing these two different patterns and probably in defining the real extent of disease.

REFERENCES

1. Kanis JA, McCloskey EV. Bisphosphonates in multiple myeloma. Cancer 2000;88(12 Suppl):3022-32.
2. Hortobagyi GN. Moving into the future: treatment of bone metastases and beyond. Cancer Treat Rev 2005;31(Suppl 3):9-18.
3. Rogers MJ, Gordon S, Benford HL, Coxon FP, Luckman SP, Monkkonen J, et al. Cellular and molecular mechanisms of action of bisphosphonates. Cancer 2000;88(12 Suppl):2961-78.
4. Coleman RE. Bisphosphonates in breast cancer. Ann Oncol 2005;16:687-95.
5. Stepensky D, Kleinberg L, Hoffman A. Bone as an effect compartment: models for uptake and release of drugs. Clin Pharmacokinet 2003;42:863-81.
6. Green JR. Antitumor effects of bisphosphonates. Cancer 2003; 97(3 Suppl):840-7.
7. Santini D, Vincenzi B, Avvisati G, Dicuonzo G, Battistoni F, Gavasci M, et al. Pamidronate induces modifications of circulating angiogenetic factors in cancer patients. Clin Cancer Res 2002;8:1080-4.
8. Migliorati CA, Schubert MM, Peterson DE, Seneda LM. Bisphosphonate-associated osteonecrosis of mandibular and maxillary bone: an emerging oral complication of supportive cancer therapy. Cancer 2005;104:83-93.
9. Pogrel MA. Bisphosphonates and bone necrosis. J Oral Maxillofac Surg 2004;62:391-2.
10. Bilezikian JP. Osteonecrosis of the jaw—do bisphosphonates pose a risk? N Engl J Med 2006;355:2278-81.
11. Ruggiero SL, Mehrotra B, Rosenberg TJ, Engroff SL. Osteonecrosis of the jaws associated with the use of bisphosphonates: a review of 63 cases. J Oral Maxillofac Surg 2004;62:527-34.
12. Marx RE. Pamidronate (Aredia) and zoledronate (Zometa) induced avascular necrosis of the jaws: a growing epidemic. J Oral Maxillofac Surg 2003;61:1115-7.
13. Bagan JV, Murillo J, Jimenez Y, Poveda R, Milian MA, Sanchis JM, et al. Avascular jaw osteonecrosis in association with cancer chemotherapy: series of 10 cases. J Oral Pathol Med 2005;34: 120-3.
14. Woo SB, Hellstein JW, Kalmar JR. Systematic review: bisphosphonates and osteonecrosis of the jaws. Ann Intern Med 2006; 144:753-61.
15. Hellstein JW, Marek CL. Bisphosphonate osteochemonecrosis (bis-phossy jaw): is this phossy jaw of the 21st century? J Oral Maxillofac Surg 2005;63:682-9.
16. Tarassoff P, Csermak K. Avascular necrosis of the jaws: risk factors in metastatic cancer patients. J Oral Maxillofac Surg 2003;61:1238-9.
17. Kristensen HK. Staining of human bone marrow after decalcification. Acta Pathol Microbiol Scand 1949;26:715-8.
18. Chiandussi S, Biasotto M, Dore F, Cavalli F, Cova MA, Di Lenarda R. Clinical and diagnostic imaging of bisphosphonate-associated osteonecrosis of the jaws. Dentomaxillofac Radiol 2006;35:236-43.
19. Gay CV, Weber JA. Regulation of differentiated osteoclasts. Crit Rev Eukaryot Gene Expr 2000;10:213-30.
20. Vaananen K, Zhao H. Osteoclast function: biology and mechanisms. In: Bilezikian J, Raisz L, Rodan G, editors. Principles of bone biology. San Diego: Academic Press; 2002. p. 127-39.
21. Luckman SP, Hughes DE, Coxon FP, Russell GG, Rogers MJ. JBMR anniversary classic. Nitrogen-containing biophosphonates inhibit the mevalonate pathway and prevent post-translational prenylation of GTP-binding proteins, including Ras. Originally published in Volume 7, number 4, pp 581-9 (1998). J Bone Miner Res 2005;20:1265-74.
22. Ridley AJ, Hall A. The small GTP-binding protein rho regulates the assembly of focal adhesions and actin stress fibers in response to growth factors. Cell 1992;70:389-99.
23. Ridley AJ, Paterson HF, Johnston CL, Diekmann D, Hall A. The small GTP-binding protein rac regulates growth factor-induced membrane ruffling. Cell 1992;70:401-10.
24. Zhang D, Udagawa N, Nakamura I, Murakami H, Saito S, Yamasaki K, et al. The small GTP-binding protein, rho p21, is involved in bone resorption by regulating cytoskeletal organization in osteoclasts. J Cell Sci 1995;108(Pt 6):2285-92.
25. Aspenberg P. Osteonecrosis of the jaw: what do bisphosphonates do? Expert Opin Drug Safety 2006;5:743-5.
26. Niinikoski JH. Clinical hyperbaric oxygen therapy, wound perfusion, and transcutaneous oximetry. World J Surg 2004;28:307-11.
27. Marx RE, Sawatari Y, Fortin M, Broumand V. Bisphosphonate-induced exposed bone (osteonecrosis/osteopetrosis) of the jaws: risk factors, recognition, prevention, and treatment. J Oral Maxillofac Surg 2005;63:1567-75.

Reprint requests:

Prof. Lorenzo Lo Muzio
Via Carelli 28
71100 Foggia
Italy
llomuzio@unifg.it